Electronic Supplementary Material (ESI) for Green Chemistry.

Optimisation of the electrochemical conversion of CO_2 into formate in a flow cell configuration using a bismuth-based electrocatalyst

Matteo Miola, [a] Donatella Chillé, [b] Georgia Papanikolaou, [b] Paola Lanzafame, [b] and Paolo P. Pescarmona [a,*]

a) Chemical Engineering Group, Engineering and Technology Institute Groningen, University of Groningen, Nijenborgh 4, 9747 AG Groningen, the Netherlands. E-mail: p.p.pescarmona@rug.nl

b) Department ChiBioFarAm, University of Messina, ERIC aisbl, INSTM/CASPE, V. le F. Stagno d'Alcontres 31, 98166 Messina, Italy

Supporting information

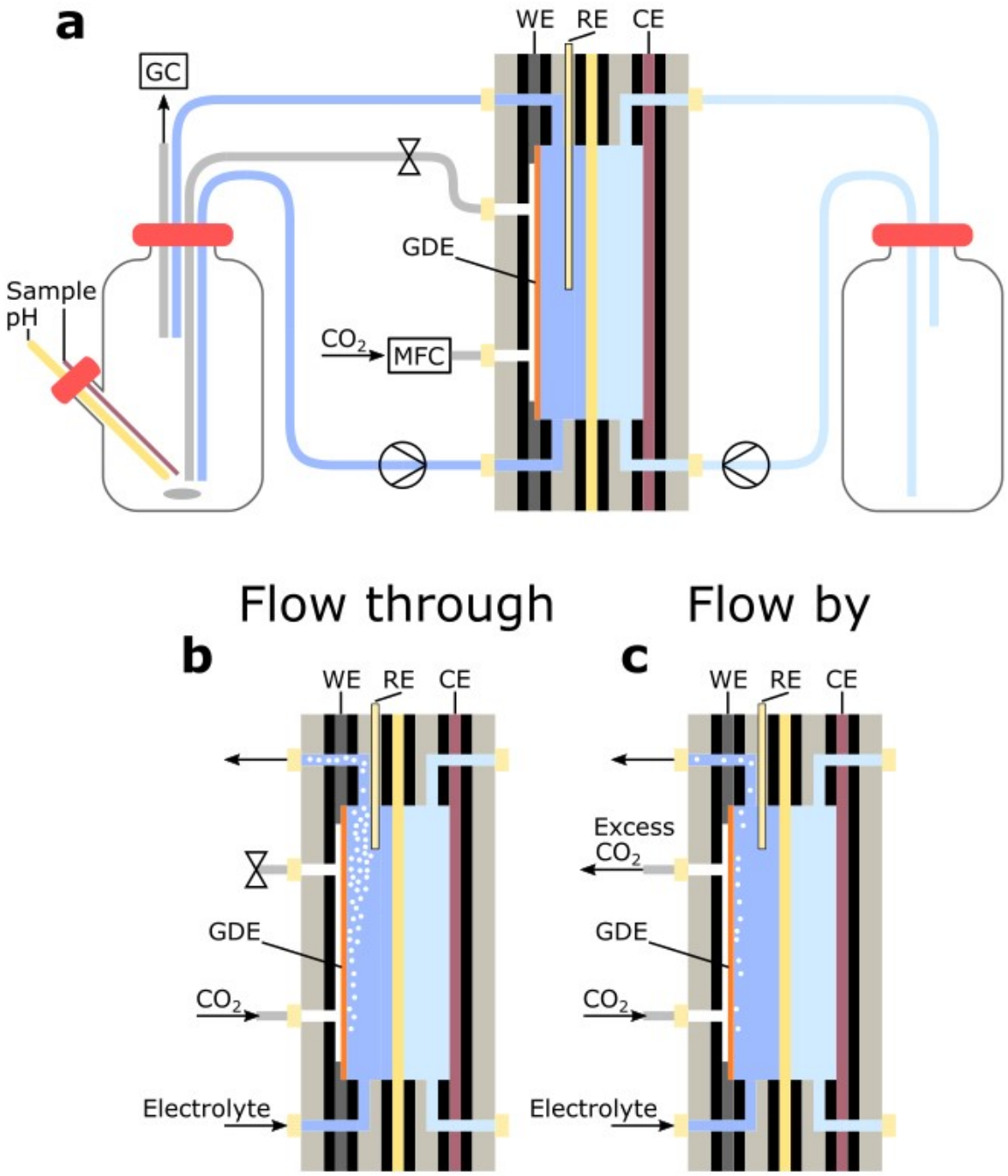

Figure S1: (a) Electrochemical flow cell system representation. CO_2 flow configurations: (b) flow through and (c) flow by.

Table S1: Literature overview on the relevant studies on CO_2 to formate electrochemical conversion in flow cell set up, with focus on multi-hour stability and bismuth-based catalysts.

Cathode El. area, Cat. load	Catholyte	Anolyte	Electrolyte Flow (mL min^{-1})	CO_2 Feed (sccm)	Membrane	$FE_{formate}$ (%)	j (A cm^{-2})	t (h)	E h.c. (V_{RHE})	E cell (V)	Ref
$Bi_{0.1}Sn$ 5 cm^2	1 M $KHCO_3$, KOH (pH 11) changed every 48 h			20-50	Sustainion X37-50	95	0.1	2400		4.3	1
	hum. CO_2	0.1 M $KHCO_3$ (pH 7.2)	15	60	Nafion TM 117	90 ->80	0.06	100		3.7 ->4.5	
2D Bi 4 cm^2, 0.4 mg cm^{-2}	hum. CO_2	0.5 M H_2SO_4	100 hum. N_2	20	PSMIM AEM, SSE-50, Nafion	83	0.03	100		2.8	2
nBuLi-Bi 4.75 cm^2, 0.7 mg cm^{-2}	hum. CO_2	hum. H_2	100 hum. N_2	50	styrene-DVB sulfonated, PS, Nafion	90->70	0.03	100		1.4 ->2.4	3
$Bi_2O_2CO_3$-NS	1 M KOH		10	50	Fumasep FAB-PK-130	93	0.2	24	-0.69 ->1.21		4
Bi-NSs 5.25 cm^2, 1.0 mg cm^{-2}		1 M KOH	10	80	Selemion	86	0.198	25	-0.51		5
NTD-Bi 16 cm^2, 1 mg cm^{-2}	1 M KOH		10	80	Selemion	95	0.14	13	-0.85		6
Leafy Bi-NS 4 cm^2		1 M KOH	7.5	20	Fumasep FAA-3-PK-130	90	0.197	10	-0.52		5
BOON Bi-2D 6.25 cm^2 1 mg cm^{-2}	0.5 M $KHCO_3$	0.5 M KOH	10	50	Nafion	80	0.2	4		6.5	7
			20	50	BPM	12	0.2	4		6.8	
Bi-ene 1 cm^2, 0.8 mg cm^{-2}		1 M KOH	9	45	BPM	99	0.2	1	-0.75		8
Sn NPs 5 cm^2, 5 mg cm^{-2}	hum. CO_2	DI	0.1 DI	20	Sustanion X37, Amberlite IR120, Nafion 324	94	0.14	142		3.4	9
Sn/C 25 cm^2, 2 mg cm^{-2}	hum. CO_2 (343 k)	1 M KOH	10	300	Nafion 115	91	0.038	48		2.2	10
SnO_2 25 cm^2, 0.5 mg cm^{-2}	0.4 M K_2SO_4 (60 °C)	KOH	40	80	BPM	100 ->80	0.15	11		4	11
BDD 0.1% 16.4 cm^2	0.5 M KCl (1L) CO_2 sat. Start/stop	0.5 M K_2SO_4 (1 L)	3.1		Nafion NRE-212	96	0.15 -> 0.2	4	-2.5 V vs Ag		12

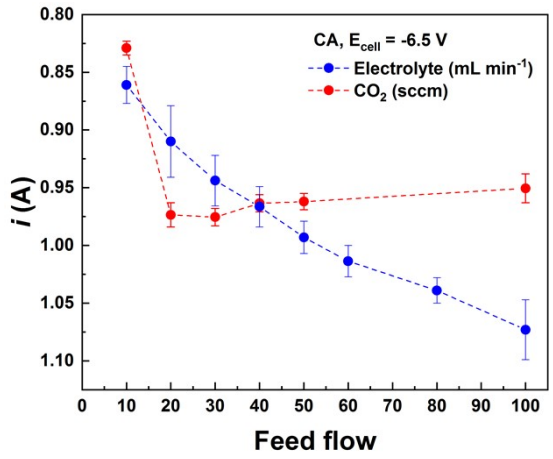

Figure S2: Current (i) dependence on electrolyte flow (blue) at constant 50 sccm CO_2 feed flow and CO_2 feed flow (red) at constant 50 mL min^{-1} electrolyte flow, in a BiSub@AC-400 equipped flow cell in CA mode at E_{cell} = -6.5 V.

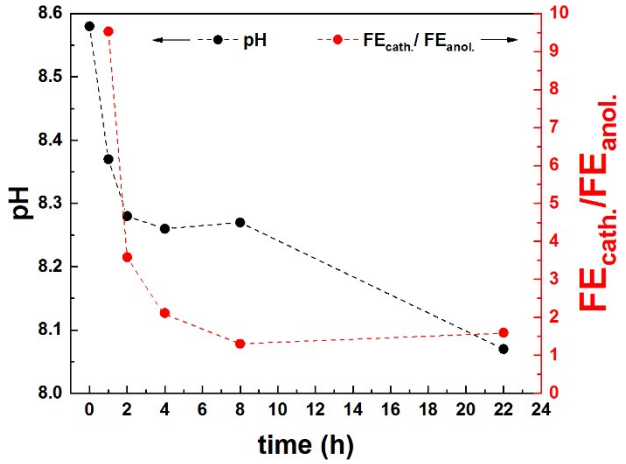

Figure S3: Chronopotentiometry at i = 1 A (100 mA cm^{-2}) with AEM (Fumatech) and 0.5 M $KHCO_3$ both as catholyte and anolyte. Catholyte pH (black dots) and Faradaic efficiency towards formate from catholyte over anolyte ratio (red dots).

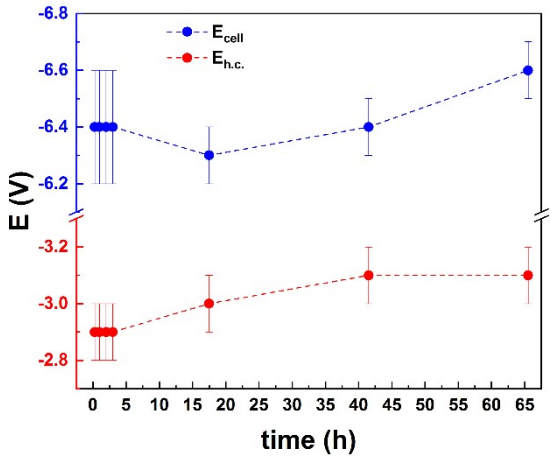

Figure S4: chronopotentiometry at i = 1 A (100 mA cm^{-2}), 0.5 M $KHCO_3$ as catholyte and 0.5 M H_2SO_4 as anolyte. E_{cell} (blue dots) and $E_{h.c.}$ (red dots).

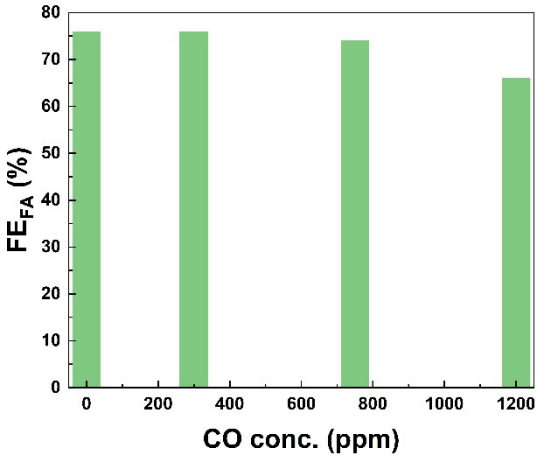

Figure S5: $FE_{formate}$ vs CO conc. in 10 mL min^{-1} CO_2 stream at E = -1.6 V vs. Ag/AgCl (chronoamperometric mode, j = 10 mA cm^{-2}) for 5 h.

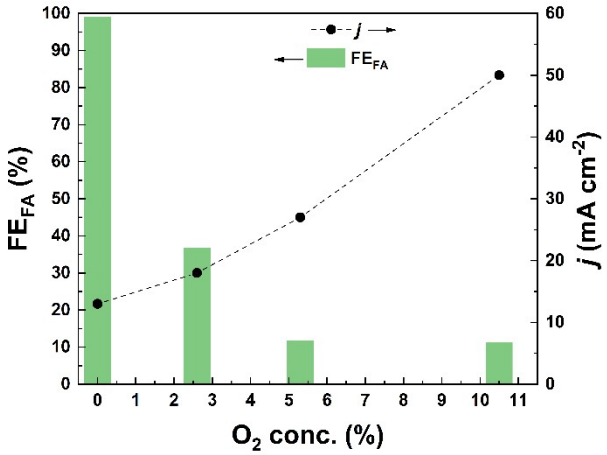

Figure S6: $FE_{formate}$ vs O_2 conc. in a 10 mL min^{-1} CO_2 stream at E= -1.6 V vs. Ag/AgCl for a total charge of 2 kC (chronoamperometric mode).

Table S2: Indicative flue gas composition at TITAN cement plant.

Flue gas composition	**Max. conc. (%vol.)**
CO_2	16
O_2	**14**
H_2O	12
N_2	Balance
Trace compounds	**Max. conc. (mg m^{-3})**
CO	**1250**
NO_x	250
SO_2	25
NH_3	15
N_2O	10
Dust	5
HCl	2
HF	0.20
Metals (Hg, Cd, Tl, As, Co, Cr, Cu, Mn, Ni, Pb, Sb, V)	0.11
PAHs	0.06

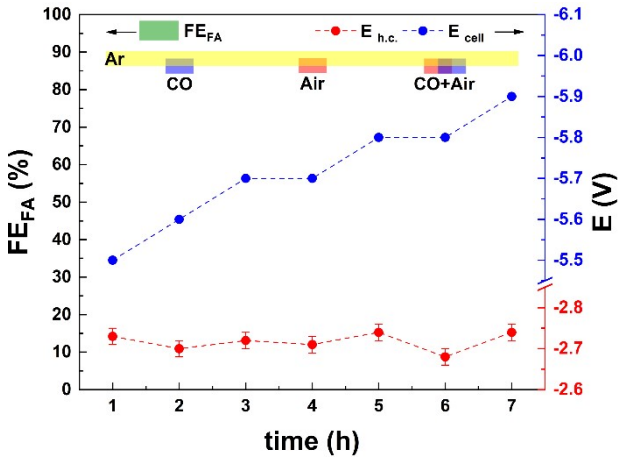

Figure S7: Gas contamination test (Ar in yellow, CO in blue, Air in orange) with chronopotentiometry at i = 1 A (100 mA cm^{-2}) for 7 h, 0.5 M $KHCO_3$ as catholyte and 0.5 M H_2SO_4 as anolyte. $FE_{formate}$ (green bars), E_{cell} (blue dots) and $E_{h.c.}$ (red dots).

Table S3: ICP analysis of the Bi content of the electrolyte after 10 h at 1 A for the BiSub@AC-400 loaded GDEs untreated, treated with 0.5 M HCOOH or HCOOK, and the 0.5 M HCOOH and HCOOK treating solution after use. The maximum Bi concentration can be 70.6 ppm in the treatment solution and 18.1 ppm in the electrolyte.

Sample	Average Bi concentration (ppm)
10 h 1 A BiSub@AC-400/GDE (0.5 M $NaHCO_3$)	< 10
HCOOH treatment solution (0.5 M HCOOH)	68.4 ± 0.1
10 h 1 A HCOOH-treated BiSub@AC-400/GDE (0.5 M $NaHCO_3$)	< 10
HCOOK treatment solution (0.5 M HCOOK)	< 10
10 h 1 A HCOOK-treated BiSub@AC-400/GDE (0.5 M $NaHCO_3$)	< 10

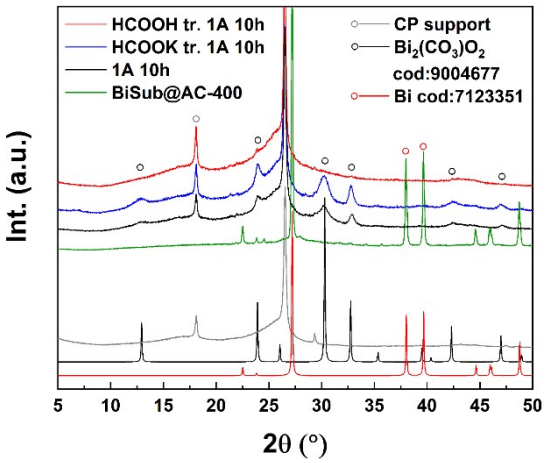

Figure S8: XRD characterisation of BiSub@AC-400 loaded GDE (green), after chronopotentiometry at 1 A for 10 h (black), with 0.5 M HCOOK pre-treatment (blue) or with 0.5 M HCOOH pre-treatment (red) and references materials: carbon paper (CP) support, $Bi_2(CO_3)O_2$ and Bi^0.

Turnover frequency (*TOF*)

The quantification of the *TOF* for heterogeneous electrocatalysts requires estimating the number of catalytically active sites. It has been proposed that the TOF can be calculated as: [13]

$$TON = \frac{n_{cycles}}{n_{catalytic\ sites}}, \qquad TOF = \frac{TON}{time}, \qquad TOF = \frac{j}{F \times n \times S}$$

where *j* is the current density [A m^{-2}], *F* the Faraday constant (96485 C mol^{-1}), *n* the number of electrons transferred to generate one molecule of the product (*n* = 2), *S* the surface concentration of active sites [m^{-2}].

The amount of electrocatalytic sites in the electrode (BiSub@AC-400 on carbon paper) was estimated by cyclic voltammetry (CO_2-saturated 0.5 M $KHCO_3$, scan rate: 10 mV s^{-1}, flow cell, Area: 10 cm^2, see Fig. S9). With the integration of the oxidation and reduction peaks and considering the scan rate of 10 mV s^{-1}, we obtained Q_{ox} = 0.616 C and Q_{red} = 0.430 C, respectively. The redox couple analysed in Fig. S9 is assigned to the Bi(III)-Bi(0) couple (number of exchanged electrons = 3). [14] The number of active sites available for the catalysis (*S*) is therefore estimated as:

$$S = \frac{Q_{red}}{F \times 3 \times 10\ cm^2} = 1.486 \times 10^{-7}\ mol\ cm^{-2}$$

Considering that the electrocatalyst loading is 0.5 mg cm^{-2}, that the electrode exposed geometric area is 10 cm^2, and that the bismuth catalyst loading is 47 wt%, [15] the total amount of bismuth on the electrode is estimated to be 2.35 mg, which corresponds to 1.12 $\times$ 10^{-6} mol_{Bi} cm^{-2}. Hence, we can estimate that ca. 13 % [(1.486 $\times$ 10^{-7} mol_{Bi} cm^{-2}/1.12 $\times$ 10^{-6} mol_{Bi} cm^{-2}) $\times$ 100%] of the Bi atoms act as electrocatalytic sites.

The *TOF* can then be calculated as follows:

$$TOF = \frac{j}{F \times n \times S} = \frac{0.1\ A\ cm^{-2}}{96485\ A\ s\ mol^{-1} \times 2 \times 1.486 \times 10^{-7}\ mol\ cm^{-2}} =$$

$$\frac{0.1}{96485 \times 2 \times 1.486 \times 10^{-7}}\ s^{-1} = 3.49\ s^{-1}$$

From which we can obtain the *TOF* towards formate by multiplying the TOF value by the $FE_{formate}$:

$$TOF_{formate} = 3.49\ s^{-1} \times FE_{formate}$$

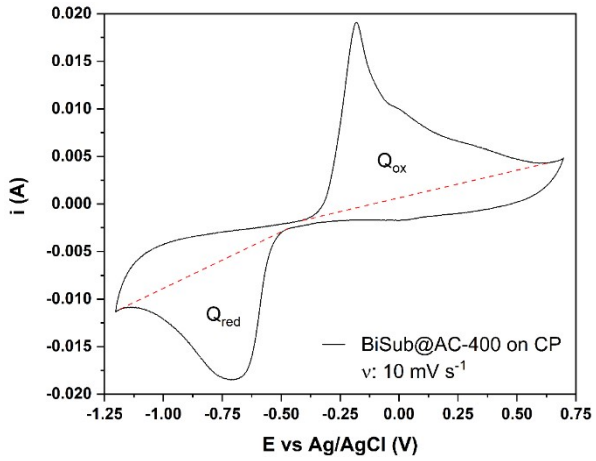

Figure S9: Cyclic voltammetry of the Bi(III)-Bi(0) redox couple obtained with the BiSub@AC-400/CP electrode at 10 mV s^{-1} in a flow cell set up (CO_2-sat 0.5 $KHCO_3$, 50 mL min^{-1}).

References

1. L. Li, A. Ozden, S. Guo, A. d. A. F. P. Garci, C. Wang, M. Zhang, J. Zhang, H. Jiang, W. Wang, H. Dong, D. Sinton, E. H. Sargent and M. Zhong, *Nat. Commun.*, 2021, **12**, 5223.
2. C. Xia, P. Zhu, Q. Jiang, Y. Pan, W. Liang, E. Stavitski, H. N. Alshareef and H. Wang, *Nat. Energy*, 2019, **4**, 776-785.
3. L. Fan, C. Xia, P. Zhu, Y. Lu and H. Wang, *Nat. Commun.*, 2020, **11**, 3633.
4. T. Fan, W. Ma, M. Xie, H. Liu, J. Zhang, S. Yang, P. Huang, Y. Dong, Z. Chen and X. Yi, *Cell Rep.*, 2021, **2**, 100353.
5. J. Yang, X. Wang, Y. Qu, X. Wang, H. Huo, Q. Fan, J. Wang, L. M. Yang and Y. Wu, *Adv. Energy Mater.*, 2020, **10**, 2001709.
6. Q. Gong, P. Ding, M. Xu, X. Zhu, M. Wang, J. Deng, Q. Ma, N. Han, Y. Zhu, J. Lu, Z. Feng, Y. Li, W. Zhou and Y. Li, *Nat. Commun.*, 2019, **10**, 2807.
7. J. Kirner, Y. Chen, H. Liu, J. Song, J. Liao, W. Li and F. Zhao, *J. Electrochem. Soc.*, 2022, **169**.
8. C. Cao, D. D. Ma, J. F. Gu, X. Xie, G. Zeng, X. Li, S. G. Han, Q. L. Zhu, X. T. Wu and Q. Xu, *Angew. Chem. Int. Ed. Engl.*, 2020, **59**, 15014-15020.
9. H. Yang, J. J. Kaczur, S. D. Sajjad and R. I. Masel, *J. CO2 Util.*, 2017, **20**, 208-217.
10. W. Lee, Y. E. Kim, M. H. Youn, S. K. Jeong and K. T. Park, *Angew. Chem. Int. Ed. Engl.*, 2018, **57**, 6883-6887.
11. Y. Chen, A. Vise, W. E. Klein, F. C. Cetinbas, D. J. Myers, W. A. Smith, T. G. Deutsch and K. C. Neyerlin, *ACS Energy Lett.*, 2020, **5**, 1825-1833.
12. Irkham, S. Nagashima, M. Tomisaki and Y. Einaga, *ACS Sustain. Chem. Eng.*, 2021, **9**, 5298-5303.
13. S. Anantharaj, P. E. Karthik and S. Noda, *Angew. Chem. Int. Ed. Engl.*, 2021, **60**, 23051-23067.
14. P. Lamagni, M. Miola, J. Catalano, M. S. Hvid, M. A. H. Mamakhel, M. Christensen, M. R. Madsen, H. S. Jeppesen, X. M. Hu, K. Daasbjerg, T. Skrydstrup and N. Lock, *Adv. Funct. Mater.*, 2020, **30**.
15. M. Miola, B. C. A. de Jong and P. P. Pescarmona, *Chem. Commun.*, 2020, **56**, 14992-14995.